Brain Imaging and Behavior (2022) 16:324–335
https://doi.org/10.1007/s11682-021-00506-8

ORIGINAL RESEARCH

Disrupted functional connectivity in white matter resting-state networks in unilateral temporal lobe epilepsy

Xuan Li[1] · Yuchao Jiang[1] · Wei Li[2] · Yingjie Qin[2] · Zhiliang Li[1] · Yan Chen[1] · Xin Tong[2] · Fenglai Xiao[2] · Xiaojun Zuo[1] · Qiyong Gong[3] · Dong Zhou[2] · Dezhong Yao[1] · Dongmei An[2] · Cheng Luo[1]

Accepted: 14 July 2021 / Published online: 3 September 2021

Abstract

Unilateral temporal lobe epilepsy (TLE) is the most common type of focal epilepsy characterized by foci in the unilateral temporal lobe grey matters of regions such as the hippocampus. However, it remains unclear how the functional features of white matter are altered in TLE. In the current study, resting-state functional magnetic resonance imaging (fMRI) was performed on 71 left TLE (LTLE) patients, 79 right TLE (RTLE) patients and 47 healthy controls (HC). Clustering analysis was used to identify fourteen white matter networks (WMN). The functional connectivity (FC) was calculated among WMNs and between WMNs and grey matter. Furthermore, the FC laterality of hemispheric WMNs was assessed. First, both patient groups showed decreased FCs among WMNs. Specifically, cerebellar white matter illustrated decreased FCs with the cerebral superficial WMNs, implying a dysfunctional interaction between the cerebellum and the cerebral cortex in TLE. Second, the FCs between WMNs and the ipsilateral hippocampus (grey matter foci) were also reduced in patient groups, which may suggest insufficient functional integration in unilateral TLE. Interestingly, RTLE showed more severe abnormalities of white matter FCs, including links to the bilateral hippocampi and temporal white matter, than LTLE. Taken together, these findings provide functional evidence of white matter abnormalities, extending the understanding of the pathological mechanism of white matter impairments in unilateral TLE.

Keywords Temporal lobe epilepsy · fMRI · White matter functional networks · Functional connectivity · Lateralization

Introduction

Temporal lobe epilepsy (TLE) is the most common type of focal epilepsy (Tellez-Zenteno & Hernandez-Ronquillo, 2012), with the temporal structures primarily involved in the genesis and propagation of interictal epileptic discharges (IED) and seizures (McIntyre & Gilby, 2008; Umeoka et al., 2012), as well as widespread cortical subcortical dysfunction far beyond the temporal lobe. Many studies have shown that TLE involves not only dysfunction in the epileptogenic zone, but also relates to disturbances with the ipsilateral and contralateral hemispheres (Cataldi et al., 2013; Morgan et al., 2019). In addition, magnetic resonance imaging (MRI) studies have found that patients with TLE have structural and functional abnormalities, i.e., hippocampal atrophy and abnormal activity and connections in the cortex (Bernhardt et al., 2016; Wei et al., 2016). These studies demonstrate that the hippocampus is considered a key component in the abnormalities of TLE and may produce widespread brain regions or network changes. However, these studies focus more on grey matter and lack data on white matter functional networks.

Although diffusion tensor imaging (DTI) has been widely used to characterize the architecture of white matter, it cannot detect neural activity inside the white matter. Using DTI

Xuan Li and Yuchao Jiang have contributed equally to this work.

✉ Cheng Luo
chengluo@uestc.edu.cn

[1] The Clinical Hospital of Chengdu Brain Science Institute, MOE Key Lab for Neuroinformation, Center for Information in Medicine, School of Life Science and Technology, University of Electronic Science and Technology of China, Second North Jianshe Road, Chengdu 610054, People's Republic of China

[2] Department of Neurology, West China Hospital, Sichuan University, Chengdu 610054, People's Republic of China

[3] Huaxi MR Research Center, Department of Radiology, West China Hospital, Sichuan University, Chengdu 610054, People's Republic of China

in TLE, previous studies observed volumetric differences in the corpus callosum, uncinate fasciculus and inferior/superior longitudinal fasciculus, decreased fractional anisotropy (FA) and increased mean diffusivity (MD) in widespread tracts (Diehl et al., 2008; Xu et al., 2018). Furthermore, accumulated works have illustrated functional activation in white matter regions corresponding to stimuli in multiple tasks such as perceptual, language and motor tasks (Fabri et al., 2011; Gawryluk et al., 2014). For example, functional MRI (fMRI) signal activity was detected not only in the primary sensory cortex, but also in the white matter fibre bundles from the somatosensory system during tactile stimulations tasks (Wu et al., 2017). Indeed, the functional organization of white matter in resting-state has been receiving increased attention. As Ding et al. note, the blood oxygenation level-dependent (BOLD) signals of white matter are relevant in neural modulation and information processing (Ding et al., 2018). Marussich et al. demonstrated that resting-state fMRI signals in white matter contain information related to brain activity and functional connectivity (Marussich et al., 2017). In addition, intrinsic functional organization has also been observed in white matter, in which several functional networks correspond with DTI tracts and are significantly correlated with grey matter functional networks (Peer et al., 2017). Using resting-state fMRI, previous studies have demonstrated white matter dysfunctional connectivity in brain disorders such as schizophrenia and Parkinson's disease (Fan et al., 2019; Ji et al., 2019; Jiang et al., 2019c; Li et al., 2019b). Our previous study in benign epilepsy with centrotemporal spikes manifested that the Rolandic area with increased white matter FC may suggest an excessive information exchange, and frontal area with the reduce white matter FC may be responsible for cognitive impairments. Therefore, it is meaningful to explore the changes in white matter functional networks, and contribute to the understanding of the pathological mechanisms in TLE.

In this study, we aimed to explore the functional activation in white matter networks (WMNs) in unilateral TLE. Based on our previous studies (Jiang et al., 2019b, c), we divided white matter into several WMNs to evaluate the functional connectivity (FC) among them. Correlations between WMNs and grey matter were also explored. Furthermore, we investigated the laterality of hemispheric WMNs in left and right TLE patients.

Methods

Participants

Seventy-one patients with left TLE (LTLE, 30 females; age: 24.89 ± 7.61 years), 79 patients with right TLE (RTLE, 35 females, age: 26.67 ± 9.01), and 47 HC (27 females, age: 29.70 ± 10.89) were recruited from West China Hospital of Sichuan University (Table 1). All patients were diagnosed with unilateral TLE according to the criteria of the International League Against Epilepsy (Engel & International League Against Epilepsy, 2001), and were evaluated by epileptologists (An and Li). A comprehensive analysis of clinical history, ictal semiology, ictal and interictal EEG, structural MRI and positron emission tomography/computed tomography (PET/CT) if available, was applied to localize the delineate the passible epileptic foci. The inclusion criteria included: (a) patients with intractable and unilateral TLE; (b) normal structural MRI other than findings of unilateral hippocampal sclerosis which was concordant to the ictal onset; (c) no evidence of bilateral hippocampal sclerosis or other lesions which may contribute to seizures; (d) any other

Table 1 Demographic and clinical information of subjects

	LTLE (N = 71)	RTLE (N = 79)	HC (N = 47)	P value
Gender (female)	30	35	27	0.146[a]
Age (years)	24.89 ± 7.61	26.67 ± 9.01	29.70 ± 10.89	0.020[b]
Age at onset (years)	13.46 ± 8.60	15.23 ± 9.51	–	0.456[c]
Duration (years)	10.97 ± 8.21	11.44 ± 8.27	–	0.693[c]
Handedness (right)	70	79	–	–
Seizure type (FS/FS, sGTCS)	27/44	31/48	–	–
Seizure frequency (daily/weekly/monthly/yearly)	7/31/28/5	8/33/30/8	–	–
History of febrile convulsions (yes)	29	28	–	–
MRI finding (HS/negative)	48/23	73/6	–	–
Number of current AEDs (0/1/2/3/4)	3/25/28/14/1	4/26/29/17/3	–	–

RTLE right TLE, *LTLE* left TLE, *HC* healthy controls, *FS* focal seizures, *sGTCS* secondary Generalized Tonic–Clonic Seizures, *HS* hippocampus sclerosis, *AEDs* antiepileptic drugs

[a]Chi-square test

[b]ANOVA, (post hoc showing patients with LTLE are younger than HC)

[c]Two-sample t test

neurologic disorders, psychological disorders or serious systematic disease. All healthy subjects confirmed that they had no history of psychiatric and/or neurological disorders. This study was reviewed and approved by the local ethics committee, and obtained written informed consent from all the subjects.

Image acquisition

Imaging data were acquired on a 3 T magnetic resonance imaging system (Siemens, Erlangen, Germany). High-resolution T1-weighted structural images were acquired by a three-dimensional fast spoiled gradient-echo (T1-3D FSPGR) sequence. The main scanning parameters include: repetition time (TR) = 1900 ms; echo time (TE) = 2.26 ms; field of view (FOV) = 256 × 256 mm^2; matrix = 512 × 512; slice thickness = 1 mm; voxel size = 1 × 1 × 1mm^3; flip angle = 9°; number of slices = 176. Resting-state functional images were obtained using a gradient-echo echo-planar imaging (EPI) sequence. The scan parameters were as follows: TR = 2000 ms; TE = 30 ms; FOV = 240 × 240 mm^2; matrix = 64 × 64; slice thickness = 5 mm (no gap); voxel size = 3.75 × 3.75 × 5 mm^3; flip angle = 90°. A total of 200 volumes were acquired for each subject and the first five time points were removed for signal equilibrium and to allow the participants to adapt at to the scanning noise. Patients were instructed to remain awake, close their eyes and think about nothing.

Data preprocessing

The analysis pipeline was similar with our prior studies (Jiang et al., 2018; Klugah-Brown et al., 2019a) and is briefly described here. The preprocessing steps included: (1) Slice-time correction. (2) Realignment. Participants with maximum motion > 2 mm or 2° were excluded from further analyses. (3) Removal of linear trends. (4) Regressed out nuisance signals of 24 motion parameter and cerebrospinal fluid. (5) Spatial smoothing on the white matter and grey matter respectively to avoid the mixture between white and grey matter signals. In detail, the individual T1images were segmented into white matter, grey matter and cerebrospinal in native space. The segmented T1 images were coregistered to the functional space for each participant to identify the whiter matter and the grey matter masks (the threshold was set at 0.5). The individual functional images were smoothed (full-width half-maximum [FWHM] = 4 mm) separately within the two masks. (6) Normalized to the Montreal Neurological Institute (MNI) template and resample into 3 mm cubic voxels. (7) Band filtered (0.01–0.15 Hz). All the preprocessing steps were performed by SPM12 (www.fil.ion.ucl.ac.uk/spm). In addition, as FC is sensitive to head-motion, we measured head motion indices (x, y, and z mean translation and rotation, and mean framewise displacement [FD]), and scrubbed the "bad" volume with excessive head-motion (FD > 1 mm). The analysis of variance (ANOVA) was used to compare the group-level head-motion differences among the three groups. There was no significant group difference of head-motion among the three group (All *P*s > 0.05).

Clustering analysis to obtain white matter functional networks

The clustering strategy refers to prior studies (Jiang et al., 2019b; Peer et al., 2017). Firstly, the high-resolution T1-weighted images were used to create a unified group-level white matter mask. The detailed process is followed: (1) the white matter, grey matter and cerebrospinal fluid (CSF) of each subject were obtained by segmenting the T1-weighted image; (2) the white matter, grey matter and CSF masks were obtained according to the maximum probability of each voxel from segmentation images for each subject; (3) the group-level white matter mask was created by averaging individual white matter masks across all subjects (the threshold = 60%); (4) to further correct the deep brain structures, we removed subcortical nuclei of the thalamus, putamen, globus pallidus and nucleus accumbens in the Harvard–Oxford atlas from the white matter mask (Desikan et al., 2006; Lorio et al., 2016); (5) the grey matter mask was also obtained using the same processing. (6) The group-level white matter mask was coregistered from the T1 space into the fMRI space and resampled to the same voxel size with the fMRI images, including 17,559 voxels of white matter.

Secondly, the K-means clustering algorithm was performed to obtain white matter spatial networks. As the complexity of the calculation, we used an interchanging grid strategy to subsample 17,559 voxels in the white-matter mask to 4398 nodes (Craddock et al., 2012). Pearson's correlation coefficients between each white-matter voxels and subsampled node were calculated and resulted in a correlation matrix (17,559 × 4398) for each subject and then averaged across all patients and HC. The K-means clustering (distance metric-correlation, 10 replicates) was performed on the averaged correlation matrix.

Thirdly, to obtain the optimal the number of clusters, Dice's coefficient was calculated with different K value from 2 to 22. Dice's coefficient measures the similarity between two adjacency matrices (where each cell represents whether 2 voxels belong to the same cluster in this solution). It is the ratio of twice the number of connections common to both matrices, divided by the total number of connections present in both matrices. In detail, the full correlation matrix (17,559 × 4398) was divided randomly into four folds (17,559 × 1099) and the same K-means clustering computation was performed on each fold separately. As

clustering gives random labels to clusters, it is difficult to directly measure similarity between clustering solutions using labels. To measure the similarity between the clustering results in different folds (Lange et al., 2004; Yeo et al., 2011), an adjacency matrix was calculated in each fold of cluster results and the Dice's coefficient was used to compare the similarity among the four adjacency matrices. For each number of clusters, all four adjacency matrices were compared to each other and an average Dice's coefficient was obtained. The above processes were repeated ten times, we obtained ten different Dice's coefficient because of the step of randomly divide was performed ten times. Then, the averaged was used to assess the stability of the number of clusters.

In addition to verify our study is reproducible and reliable in different sets of subjects. We randomly selected half of the subjects as the test group and the other half to verify the effects, and full group-average correlation matrices were computed for each group. K-means Clustering was separately performed on the full connectivity matrix from each subject group. The two solutions were again compared for each number of clusters using Dice's coefficient as described above.

Functional connectivity white matter networks

To investigate synchronous activation of resting-state WMNs, the FC between any two WMNs were calculated for each subject. Briefly, the average time series of voxels within each WMN were extracted. The Pearson's correlation coefficient between average time series was calculated and then transformed to the Fisher's z-score. In addition, to determine functional interaction between white matter and grey matter, we calculated the FC between each WMN and grey matter regions, the grey matter regions used here were defined from the automated anatomical labeling (AAL) atlas (Tzourio-Mazoyer et al., 2002).

FC laterality of hemispheric white matter networks

Previous studies have demonstrated that abnormal FCs are associated with the altered hemispheric communication and propagation of interictal epileptic discharges in TLE (Kobayashi et al., 2006; Morgan et al., 2015).We investigated the intra-hemispheric and inter-hemispheric connectivity of WMNs using functional connectivity strength (FCS, which represents the sum of the functional connections for a given network). Considering that TLE has laterality, each WMN was further divided into *2*symmetricsub-networks on the basis of their location in left or right hemisphere. Naturally, we obtained $2 \times K$sub-networks for *K*WMNs. To reduce the bias of anatomical differences from the asymmetry between the hemispheres, an additional normalization step was performed by coregistering the functional images from the MNI template into a symmetrized template (Agcaoglu et al., 2015). In detail, the symmetrized template was produced by an average of template and its mirror image. Then, the functional images in MNI template was spatially normalized to the symmetrized template and this warping was applied to *K* white matter clustering networks to obtain symmetrized networks. The FC was calculated among the $2 \times K$ sub-networks for each subject. The FC values were transformed to Fisher's z scores and normalized by dividing by the mean FC z score to reduce the effect of individual variability.

For each network, the intra-hemispheric FCS is defined that the summation of FCs, which link the sub-network and other same hemispheric sub-networks.

$$\mathrm{FCS}_{LL}\left(\mathrm{WM}_i\right) = \sum_{j=1}^{K-1} \mathrm{FC}_{jL,iL} \tag{1}$$

$$\mathrm{FCS}_{RR}\left(\mathrm{WM}_i\right) = \sum_{j=1}^{K-1} \mathrm{FC}_{jR,iR} \tag{2}$$

where $\mathrm{FC}_{\mathrm{jL,iL}}$ represents the FC between left sub-network *j* and left sub-network *i*, $\mathrm{FC}_{\mathrm{jR,iR}}$ represents the FC between right sub-network *j* and right sub-network *i*; A flow-chart of FCS calculation is shown in Fig. 1.

For each network, the inter-hemispheric FCS is defined that the summation of FCs, which link the sub-network and different hemispheric sub-networks.

$$\mathrm{FCS}_{LR}\left(\mathrm{WM}_i\right) = \sum_{j=1}^{K} \mathrm{FC}_{jL,iR} \tag{3}$$

$$\mathrm{FCS}_{RL}\left(\mathrm{WM}_i\right) = \sum_{j=1}^{K} \mathrm{FC}_{jR,iL} \tag{4}$$

where $\mathrm{FC}_{\mathrm{jL,iR}}$ represents the FC between left sub-network *j* and right sub-network *i*; $\mathrm{FC}_{\mathrm{jR,iL}}$ represents the FC between right sub-network *j* and left sub-network *i*; A flow-chart of FCS calculation is shown in Fig. 1.

To further describe the laterality of FCS of WMNs in the TLE, we calculated the intra-hemisphere LI ($\mathrm{LI}_{\mathrm{intra}}$) and inter-hemisphere LI ($\mathrm{LI}_{\mathrm{inter}}$) for each WMN.

$$LI_{intra}\left(\mathrm{WM}_i\right) = \frac{\mathrm{FCS}_{LL}\left(\mathrm{WM}_i\right) - \mathrm{FCS}_{RR}\left(\mathrm{WM}_i\right)}{\mathrm{FCS}_{LL}\left(\mathrm{WM}_i\right) + \mathrm{FCS}_{RR}\left(\mathrm{WM}_i\right)} \tag{5}$$

$$LI_{inter}\left(\mathrm{WM}_i\right) = \frac{\mathrm{FCS}_{LR}\left(\mathrm{WM}_i\right) - \mathrm{FCS}_{RL}\left(\mathrm{WM}_i\right)}{\mathrm{FCS}_{LR}\left(\mathrm{WM}_i\right) + \mathrm{FCS}_{RL}\left(\mathrm{WM}_i\right)} \tag{6}$$

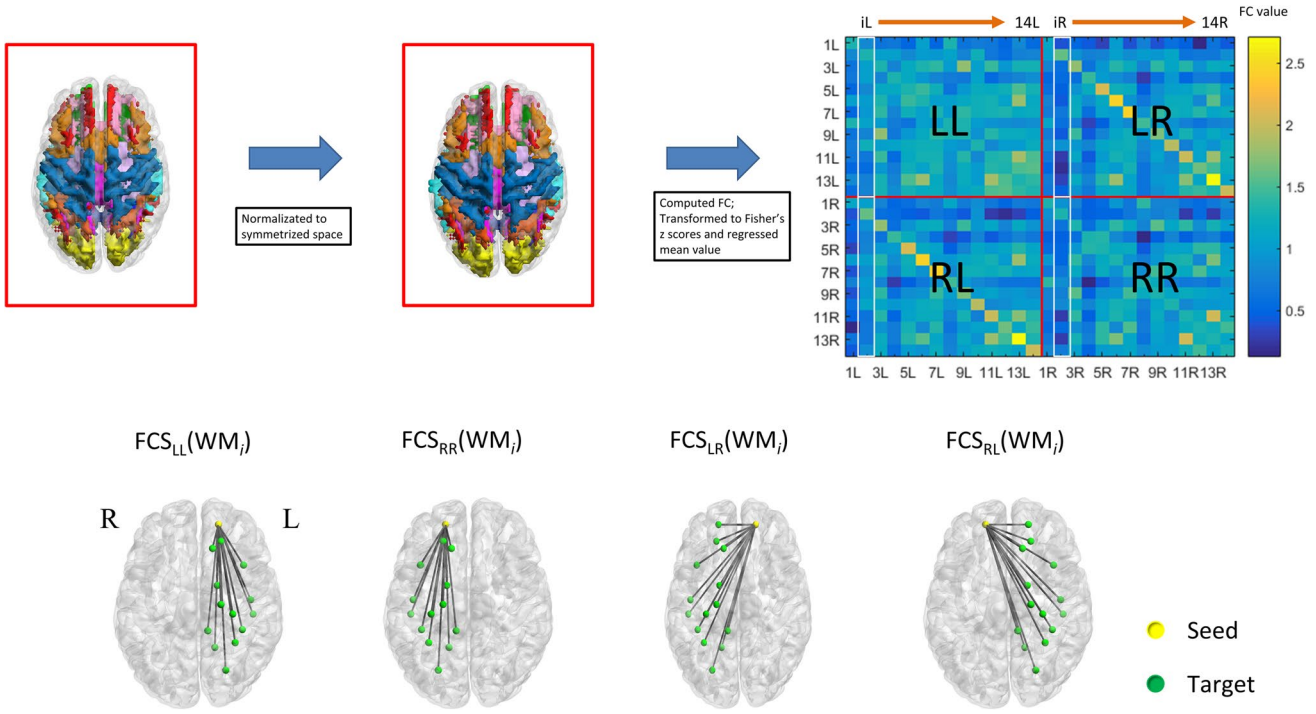

Fig. 1 A flow-chart of Functional connectivity strength (FCS). First, the original white matter networks were normalized to symmetry space, then the *K* white matter networks were divided into *2K* symmetry sub-networks. Second, the FC was calculated to acquire a matric (2k*2k). The FCS was used to estimate the hemispheric connectivity of each white matter network by summing the FCs (bottom row). Here, $FCS_{LL}(WM_i)$ represents the summation the FC values between left hemisphere sub-network *i* and the remained left white matter sub-networks. $FCS_{LR}(WM_i)$ represents the summation the FC values between left hemisphere sub-network *i* and right white matter sub-networks

where all of the components of the right side of the formula were described above and explained in detail. Finally, the LI_{intra} and LI_{inter} values were further transformed into Fisher's z-scores to allow for normalization. Positive intra-hemisphere (inter-hemisphere) LI values indicate a higher intra-hemisphere (inter-hemisphere) FCS in the left hemisphere, and negative intra-hemisphere (inter-hemisphere) LI values indicate a higher intra-hemisphere (inter-hemisphere) FCS in the right hemisphere.

Statistical analysis

One-sample t tests were performed for the FCs to evaluate the synchronous activation in white-matter among the LTLE group, RTLE group and HC group. Then, to obtain the difference among three groups ANOVA was performed with age as a covariate. Multiple comparisons correction was performed using the FDR with $q < 0.05$. Post hoc analysis was further used to compare the differences between any two groups. For FCS and LI, ANOVA and post hoc tests were performed to compare the differences among the three groups.

Results

Clustering analysis of functional networks in the white matter

According to the Dice's coefficients (> 0.85), $K = 14$ was the optimal value among 2–22 for the clustering analysis of functional networks in the white matter (Fig. 2). The fourteen WMNswereWM1 (temporofrontal network), WM2 (temporal network), WM3 (orbitofrontal network), WM4 (prefrontal network), WM5 (occipital network), WM6 (cerebellar network), WM7 (precentral/postcentral network), WM8 (anterior corona radiate network), WM9 (temporoparietal network), WM10 (posterior corpus callosum network), WM11 (anterior corpus callosum network), WM12 (superior corona radiate network), WM13 (intracerebral capsule network) and WM14 (superior longitudinal fasciculus network). According to their spatial locations, the clustered WMNs can be divided into three layers (superficial, middle and deep) (Fig. 3). Interestingly, WM2 locate in the bilateral temporal lobe that is linked to the epileptogenic zone in TLE.

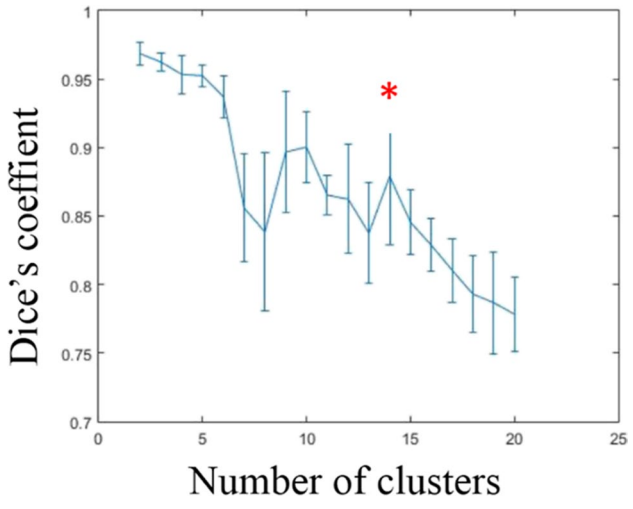

Fig. 2 Stability of clustering for different of clusters, measured by Dice's coefficient

Functional connectivity between white matter networks

Seventeen FCs between WMNs showed significant group differences among the LTLE, RTLE and HC groups by the ANOVA ($q < 0.05$, FDR corrected). In detail, seven links were observed among the superficial WMNs: WM2-WM4, WM2-WM6, WM2-WM8, WM5-WM6, WM6-WM7, WM6-WM8 and WM6-WM9. The FCs of WM2-WM13, WM5-WM11, WM7-WM11, WM8-WM13 and WM9-WM11 were included, which represent the connections of superficial and middle WMNs. Altered FCs between superficial and deep WMNs were observed inWM7-WM14 and WM9-WM14. Among the different middle networks, only the FC between WM11 and WM12was altered. The FC of WM12-WM14 belonged to middle and deep WMN connections. Post hoc analysis further revealed that these FCs were decreased in the LTLE and RTLE groups compared with the HC group (Fig. 4a, Table. S1). Interestingly, the LTLE group had a greater FC between temporal network and prefrontal network than RTLE group.

Furthermore, thirty-five FCs between superficial WMNs and grey matter regions showed significant group differences among the LTLE, RTLE and HC groups by ANOVA. Post hoc analysis revealed that most connections were reduced in the LTLE and RTLE groups compared with HC group (Fig. 4b, Table S2). Nineteen FCs between the white matter middle networks and grey matter regions showed significant group effects among the LTLE, RTLE and HC groups. Post hoc analysis found that almost all connections were reduced in RTLE and most connections were reduced in LTLE compared with HC (Fig. 4b, Table S2). TheWM-14FCs with both the right postcentral gyrus and the right precentral gyrus showed significant group differences among the LTLE, RTLE and HC group. Post hoc analyses indicated that these FCs were lower in the LTLE group than in the HC group (Fig. 4b, Table S2). Interestingly, we found that the FCs between the right hippocampus and the superficial and middle WMNs were decreased in the RTLE group compared with the HC group.

Laterality index analysis of the white matter networks

ANOVA revealed significant group effects of FCS_{RR} inWM3 [$F = 5.09$, $P = 0.0069$] and WM6 [$F = 6.13$, $P = 0.0026$]. Post hoc analysis found reduced FCS_{RR} in WM6 for both patient groups compared with the HC group. In addition, the LTLE group had an increased FCS_{RR} in WM3 compared to the RTLE and HC groups (Fig. 5a, Table S3). For FCS_{LR}, ANOVA indicated a significant group effect in WM2 [$F = 7.8$, $P = 0.00055$] among the LTLE, RTLE and HC groups. Post hoc analysis showed a reduced FCS_{LR} in WM2 in the RTLE group compared with the other two groups (Fig. 5b, Table S3). In addition, ANOVA indicated that FCS_{RL} had significant group effects in WM3 [$F = 4.998$, $P = 0.008$], WM4 [$F = 6.949$, $P = 0.0016$], WM6 [$F = 7.91$, $P = 0.00047$] and WM11 [$F = 5.726$, $P = 0.004$]. Post hoc analysis showed increased FCS_{RL} in the LTLE group compared with the other two groups for WM3.TheRTLE group had a lower FCS_{RL} in WM4 compared with the LTLE group. ForWM6 and WM11, the LTLE and RTLE groups had lower FCS_{RL} than the HC group (Fig. 5c, Table S3).

For LI_{inter}, we found group differences in WM2 [$F = 6.176$, $P = 0.003$] and WM4 [$F = 7.815$, $P = 0.001$] among the LTLE, RTLE and HC groups by ANOVA. In detail, WM2 in the RTLE group had a decreased LI_{inter} compared with the LTLE group.WM4 had an increased LI_{inter} in the RTLE group compared with the LTLE and HC groups (Fig. 6, Table S4). In addition, there was no significant difference in LI_{intra} in all WMNs among the LTLE, RTLE and HC groups.

Validation analysis

To keep the robustness of clustering analysis, the same clustering algorithm was performed in randomly selected half of subjects. These results of clustering indicated that the clustering results are robust and do not depend on random noise or on the characteristics of specific subjects (Supplementary Fig. 1). Furthermore, we used ANOVA to test the different of FC between white matter networks among three groups in randomly selected half of the subjects and the differences of FC remained consistent with previous results (Supplementary Figs. 2, 3).

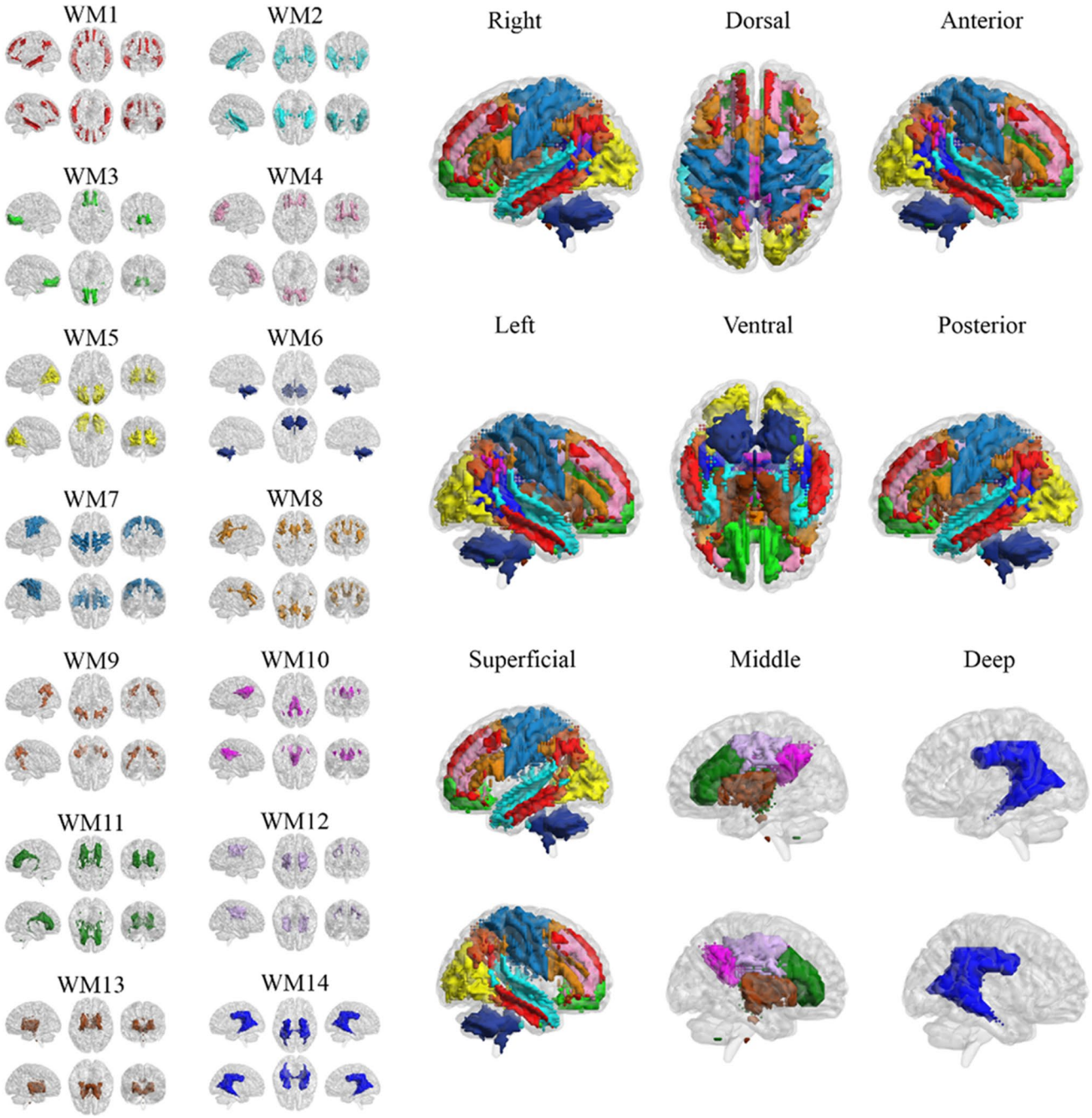

Fig. 3 White matter functional networks. The fourteen white matter functional networks are the temporofrontal network (WM1), the temporal network (WM2), the orbitofrontal network (WM3), the prefrontal network (WM4), the occipital network (WM5), the cerebellar network (WM6), the precentral/postcentral network (WM7), the anterior corona radiate network (WM8), the temporoparietal network (WM9), the posterior corpus callosum network (WM10), the anterior corpus callosum network (WM11), the superior corona radiate network (WM12), the intracerebral capsule network (WM13) and the superior longitudinal fasciculus network (WM14)

Discussion

Consistent with previous studies (Jiang et al., 2019b, c; Peer et al., 2017), we found resting-state white matter functional networks that were classified into superficial, middle and deep layers in unilateral TLE. We observed reduced FCs across WMNs as well as reduced FCs between white matter and grey matter in both LTLE and RTLE groups compared with the HC group. Interestingly, specifically altered FCs between WMNs and the bilateral hippocampi were observed in RTLE, while only the ipsilateral hippocampus was affected in LTLE. Further laterality of the hemisphere

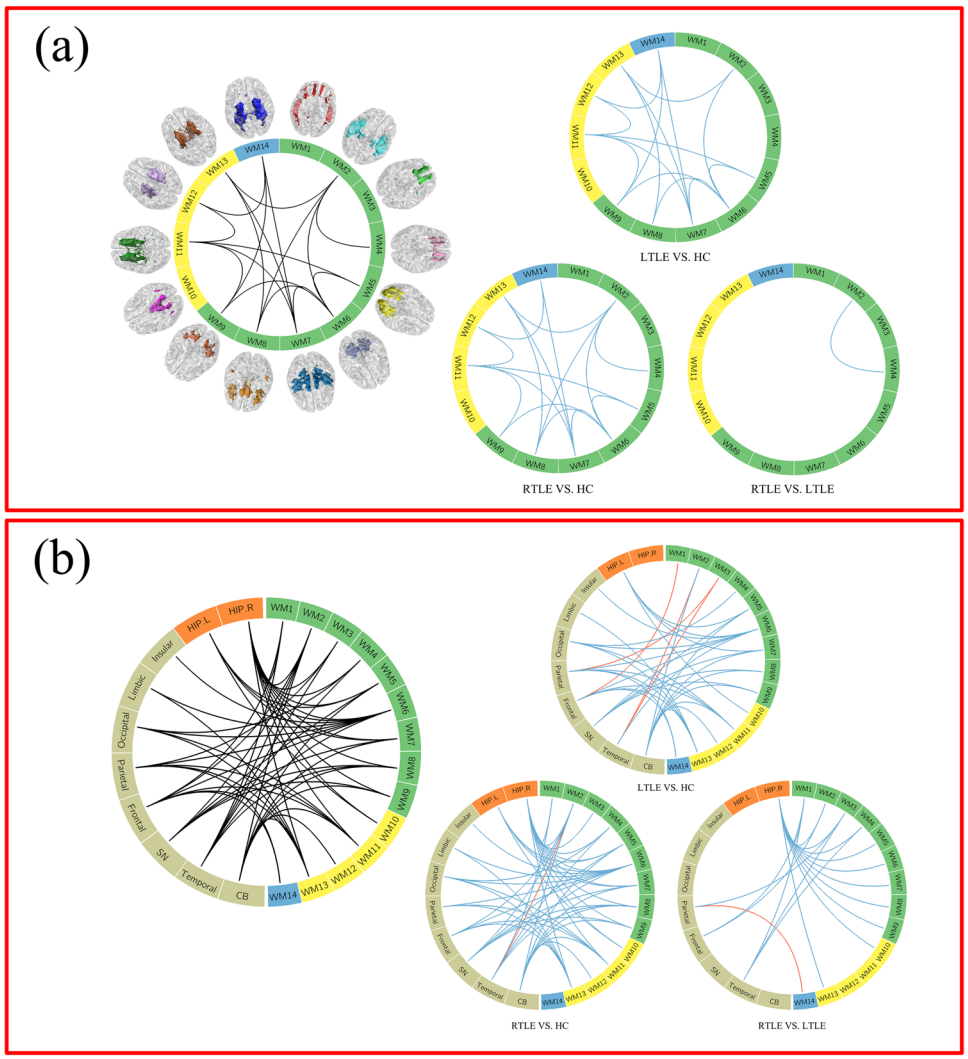

Fig. 4 Functional connectivity (FC) of the LTLE group, RTLE group and HC group were compared by analysis of variance (ANOVA) and post hoc analysis. **a** Left part showing that the FCs between white matter networks have significant differences among the three groups. Right part showing that the patient groups had a significant reduction in FC compared with the HC group. **b** Left part showing that the FCs between white matter and grey matter regions were significantly different among the three groups. Right part shows that the patient group had a significant reduction in most FCs compared with the HC group and that the right hippocampus had different roles in the two patient groups. Black lines represent significant group effects, blue lines represent decreased FCs and red lines represent increased FCs. *Note:* Green, superficial white matter networks; yellow, middle white matter networks; blue, deep white matter networks; chartreuse, grey matter; orange, hippocampus. *CB* cerebellum; *SN* subcortical nuclei; *HIP.L (R)* left (right) hippocampus

revealed common alterations in frontal and cerebellar WMNs in two patient groups and specific changes in temporal WMNs. These findings contribute to understanding the role of white matter in the pathological mechanism of unilateral TLE.

Decreased functional connectivity among the white matter networks

Previous studies have suggested that white matter FC is related to brain disorders (Ji et al., 2019; Jiang et al., 2019b, c). Consistent with previous studies (Jiang et al., 2019b; Peer et al., 2017), we observed that these WMNs can be classified into three layers (superficial, middle and deep) based on spatial location. In addition, we found altered FCs between superficial and superficial networks as well as between middle and middle networks in TLE. These connections link adjacent WMNs and thus are defined as short-range connectivity. Long-range connectivity included connections that linked superficial networks with middle networks and with deep networks. Infact, the DTI study also found abnormal long-range fibre bundle connections in TLE (Li et al., 2019a). As Diehl et al. note, the uncinate fasciculus, which is the major fibre tract connecting the frontal and temporal lobes, had significantly changed FA in TLE, suggesting a temporal to frontal abnormal pathway (Diehl et al., 2008). DeSalvo et al. reported that patients with TLE had reduced FA in widespread tracts including the uncinate, arcuate, superior longitudinal and inferior longitudinal fasciculi (DeSalvo et al., 2014). Specifically, the cerebellar white matter network (WM6) illustrated a decreased FC with the other WMNs in both patient groups especially in superficial WMNs. Recently, cerebellar damage was reported in many studies of brain disorders (He et al., 2019; Jia et al., 2019; Jiang et al., 2019a; Qin et al., 2019).For example, patients with TLE illustrated a significant reduction in anatomical volume (McDonald et al., 2008), abnormal activation (Zhou et al., 2019) and white matter dys-connectivity (Focke

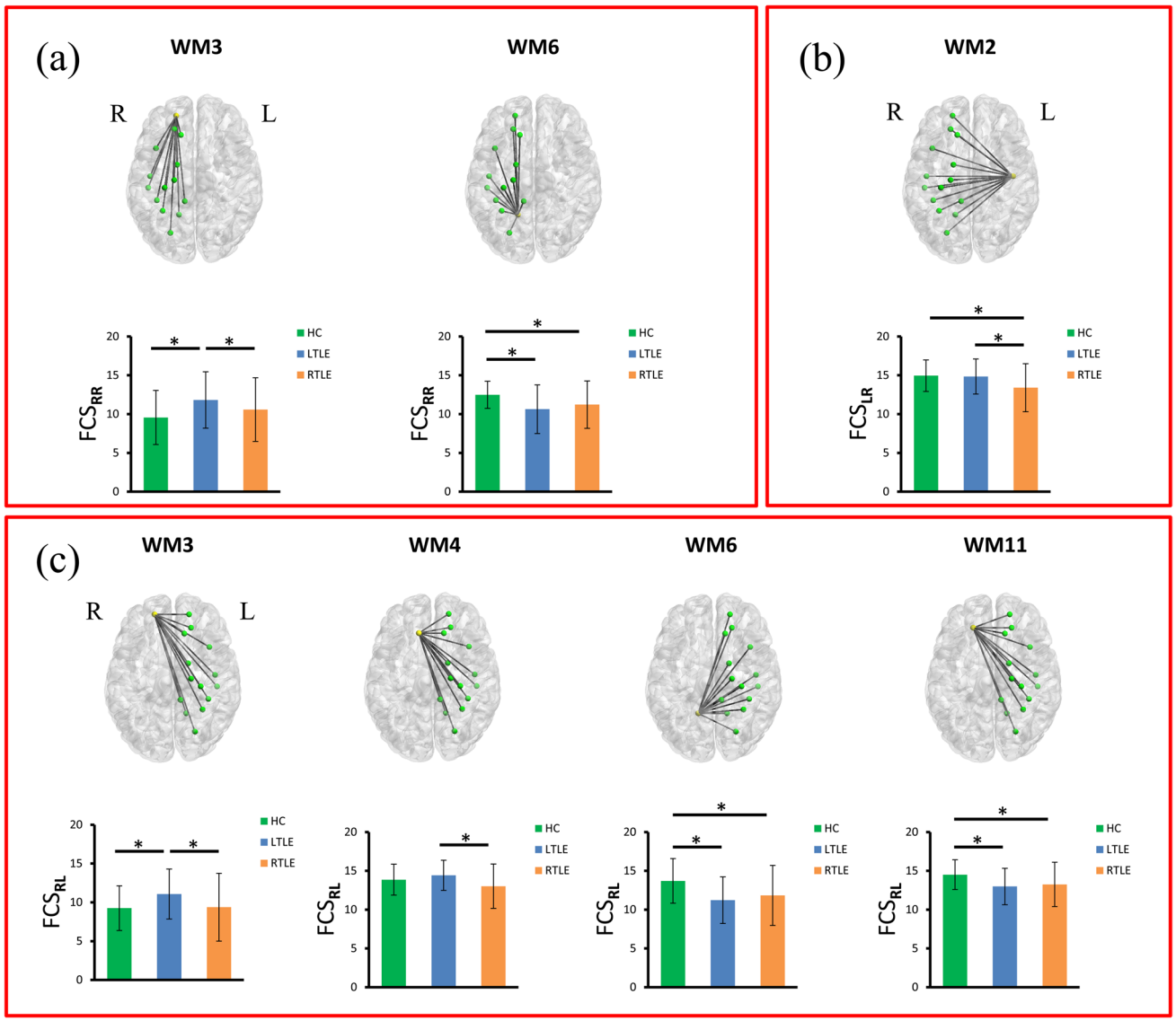

Fig. 5 Group differences of functional connectivity strength (FCS) for white matter networks among the three groups by analysis of variance (ANOVA). **a** Orbitofrontal network (WM3) and cerebellar network (WM6) showing significant differences in the right intra-hemisphere FCS (FCS_{RR}). **b** Temporal network (WM2) showing significant differences in the left inter-hemisphere FCS (FCS_{LR}). **c** Orbitofrontal network (WM3), prefrontal network (WM4), cerebellar network (WM6), and anterior corpus callosum network (WM11) showing significant differences in the right inter-hemisphere FCS (FCS_{RL})

et al., 2008). In addition, numerous studies have highlighted that the cerebellum plays an important role in the regulation of epileptic discharges (Kros et al., 2015a, b). Thus, the alterations in the cerebellar white matter may suggest a dysfunctional interaction with cerebral white matter in TLE. Combined with these structural findings, the reduced white matter FC suggests insufficient informational integration in unilateral TLE.

Informational interaction between white matter and grey matter

Resting-state fMRI in epilepsy has demonstrated widespread decreased FC in focal epilepsy patients versus controls (Klugah-Brown et al., 2019b; Voets et al., 2012; Zhu et al., 2018). For example, our previous study found decreased FC across eight resting-state grey matter networks in TLE (Luo et al., 2012). In this study, we found decreased FC between white matter and grey matter, suggesting that the abnormal functional integration was not limited to brain grey matter in unilateral TLE. In particular, FCs were decreased

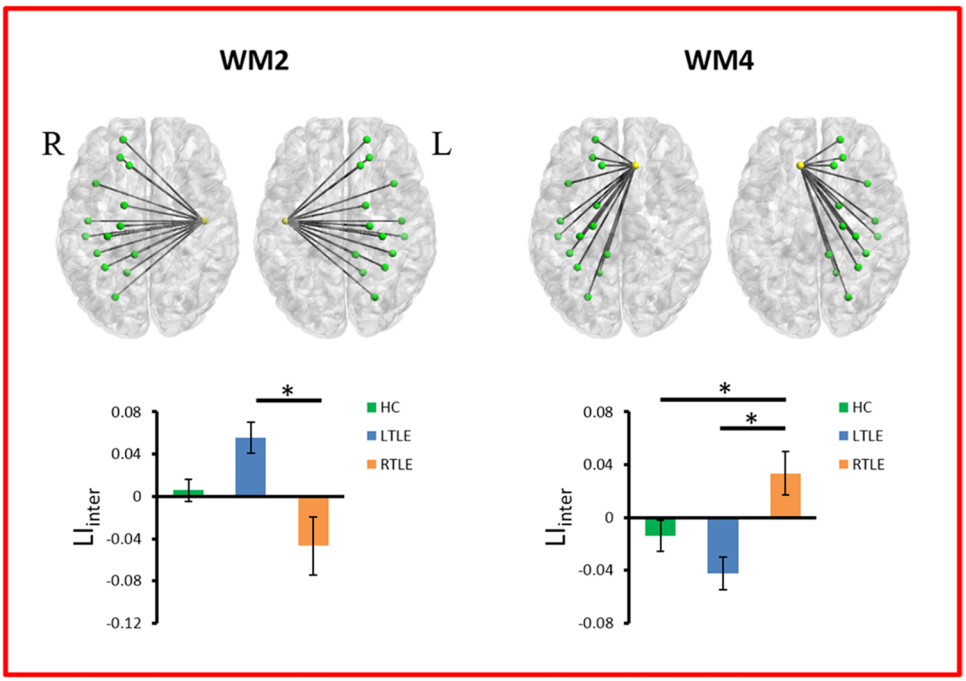

Fig. 6 Group differences in the laterality index (LI) for white matter networks among the three groups by analysis of variance (ANOVA). Temporal network (WM2) and prefrontal network (WM4) showed significant differences in the LTLE, RTLE and HC groups

between WMNs and the ipsilateral hippocampus, which is generally considered the epileptogenic focus of unilateral TLE. In addition, patients with RTLE showed a more severe decrease in FC between WMNs and bilateral hippocampi than patients with LTLE. Consistent with our findings, Voetset al. found a reduced FC not only in the ipsilateral cortices but also in the contralateral temporal lobe for RTLE; however, a decreased FC was observed in the ipsilateral temporal lobe for LTLE (Voets et al., 2012), suggesting that the abnormality was restricted to ipsilateral regions in LTLE whereas it involved bilateral regions in RTLE. Thus, we presumed that the abnormal activity of the right hippocampus might propagate easily to the left hippocampus in RTLE, which might lead to altered FCs of WMNs with the bilateral hippocampi. However, the abnormal activity was restricted in LTLE. In addition, the various alterations in right and left TLE might be related to cognitive function. Neuroimaging studies have demonstrated that changes in the hippocampus, as a key abnormal focus in TLE, result in verbal and nonverbal memory deficits (Bonilha et al., 2004; Dupont et al., 2000). Li et al. found that the decreased hippocampal FC was more extensive in RTLE than LTLE, suggesting more severe hippocampal damage associated with more memory deficits in the RTLE (Li et al., 2017). On the whole, white matter FC is also affected by epileptogenic focus in unilateral TLE. The specific change in RTLE may be related to the propagation of epileptic activity and cognitive deficits different from those in LTLE.

Hemispheric communications in white matter networks

Epilepsy is generally considered a system-level disease characterized by aberrant neuronal synchronization. Characterizing hemispheric communication in patients with epilepsy is crucial to understanding the pathophysiology of this disorder. Moreover, TLE with unilateral temporal structural abnormalities often leads to asymmetrical brain dysfunction. Here, we found disturbed hemispheric communication between ipsilateral and contralateral white matter functional networks in unilateral TLE. These abnormalities mostly existed in the right hemisphere WMNs. Interestingly, patients with RTLE showed decreased inter-hemisphere connection in the contralateral temporal white matter network (WM2) compared with LTLE. This funding implies that the left temporal white matter is also affected in RTLE. In addition, we found abnormal asymmetry in the z-scores including the orbitofrontal white matter network (WM3), the prefrontal white matter network (WM4) and the anterior corpus callosum network (WM11) in both patient groups. The inter-hemisphere FC between WMNs was more reduced in RTLE than in LTLE. The findings are in line with past studies, abnormal frontal fibre bundles were observed using DTI in TLE (Rodrigo et al., 2007). In general, the frontal lobeis associated with cognitive function (Schuck et al., 2016) and the asymmetry of the FC in frontal white matter may contribute to cognitive impairments in unilateral TLE.

Limitations

Although our research extends the understanding of the resting-state of WMNs in TLE, there are some limitations. First, it is unclear whether the altered white matter signals reflect neuron-related activity. However, Gawryluk et al. suggest that the white matter haemodynamic changes they observed may be related to spiking activity and blood vessels in white matter (Gawryluk et al., 2014). Second, the neuropsychological tests were not fully completed in the current study. In the future, we should investigate the performance of higher-level cognitive tasks to assess the association between white matter features and cognitive impairments. Alternatively, event-related fMRI might provide more evidence on the pathological mechanism of white matter impairments in TLE. Third, there was a significant difference in age among the groups (post hoc showed that patients in the LTLE group were younger than those in the HC group), which may have cause bias in the results. Although age was considered a regressor in the subsequent analysis, it nevertheless may have influenced our findings. Fourthly, in our study, white matter mask was obtained using the parcellation of grey-white matter for all subjects together. Because individual grey-white matter parcellation boundaries should be different between patients and controls, this strategy might potentially influence our results. Finally, the exact definition of clusters' number (K) is crucial ink-means clustering. Although the stability of clusters remains open, some interesting approaches were introduced to optimize the number of cluster such as the bootstrap techniques and stability calculation (Bellec et al., 2010; Kelly et al., 2012). Thus, more optimal strategies would be considered in the future.

Conclusion

The present study demonstrated reduced FC across the superficial, middle and deep WMNs in TLE. Specifically, cerebellar white matter illustrated a decreased FC with the cerebral superficial WMNs, implying a dysfunctional interaction between the cerebellum and the cerebral cortex in TLE. In addition, the FCs of WMNs and the ipsilateral hippocampus (grey matter foci) were also reduced in patient groups, which may suggest insufficient functional integration in unilateral TLE. Interestingly, RTLE showed more severe abnormalities of white matter FC, including links to the bilateral hippocampi and the temporal white matter compared to LTLE. In general, these findings provide functional evidence of white matter to extending the understanding of the pathological mechanism of white matter impairments in unilateral TLE.

Supplementary Information The online version contains supplementary material available at https://doi.org/10.1007/s11682-021-00506-8.

Acknowledgements This study was funded by grants from the National Nature Science Foundation of China (Grant Number: 61933003, 81771402, 81701076, 81771822, 81960249, 81861128001), and the '111' Project (B12027). We gratefully acknowledge the participation of the study subjects and investigators.

Declarations

Conflict of interest There is no conflict of interest.

References

Agcaoglu, O., et al. (2015). Lateralization of resting state networks and relationship to age and gender. *NeuroImage, 104*, 310–325.

Bellec, P., et al. (2010). Multi-level bootstrap analysis of stable clusters in resting-state fMRI. *NeuroImage, 51*(3), 1126–1139.

Bernhardt, B. C., et al. (2016). The spectrum of structural and functional imaging abnormalities in temporal lobe epilepsy. *Annals of Neurology, 80*(1), 142–153.

Bonilha, L., et al. (2004). Voxel-based morphometry reveals gray matter network atrophy in refractory medial temporal lobe epilepsy. *Archives of Neurology, 61*(9), 1379–1384.

Cataldi, M., Avoli, M., & de Villers-Sidani, E. (2013). Resting state networks in temporal lobe epilepsy. *Epilepsia, 54*(12), 2048–2059.

Craddock, R. C., et al. (2012). A whole brain fMRI atlas generated via spatially constrained spectral clustering. *Human Brain Mapping, 33*(8), 1914–1928.

DeSalvo, M. N., et al. (2014). Altered structural connectome in temporal lobe epilepsy. *Radiology, 270*(3), 842–848.

Desikan, R. S., et al. (2006). An automated labeling system for subdividing the human cerebral cortex on MRI scans into gyral based regions of interest. *NeuroImage, 31*(3), 968–980.

Diehl, B., et al. (2008). Abnormalities in diffusion tensor imaging of the uncinate fasciculus relate to reduced memory in temporal lobe epilepsy. *Epilepsia, 49*(8), 1409–1418.

Ding, Z. H., et al. (2018). Detection of synchronous brain activity in white matter tracts at rest and under functional loading. *Proceedings of the National Academy of Sciences of the United States of America, 115*(3), 595–600.

Dupont, S., et al. (2000). Episodic memory in left temporal lobe epilepsy: A functional MRI study. *Brain, 123*, 1722–1732.

Engel, J., Jr., & International League Against Epilepsy. (2001) A proposed diagnostic scheme for people with epileptic seizures and with epilepsy: Report of the ILAE Task Force on Classification and Terminology. *Epilepsia, 42*(6), 796–803.

Fabri, M., et al. (2011). Topographical organization of human corpus callosum: An fMRI mapping study. *Brain Research, 1370*, 99–111.

Fan, Y. S., et al. (2019). Impaired interactions among white-matter functional networks in antipsychotic-naive first-episode schizophrenia. *Human Brain Mapping, 41*(1), 230–240.

Focke, N. K., et al. (2008). Voxel-based diffusion tensor imaging in patients with mesial temporal lobe epilepsy and hippocampal sclerosis. *NeuroImage, 40*(2), 728–737.

Gawryluk, J. R., Mazerolle, E. L., & D'Arcy, R. C. N. (2014). Does functional MRI detect activation in white matter? A review of emerging evidence, issues, and future directions. *Frontiers in Neuroscience*. https://doi.org/10.3389/fnins.2014.00239

He, H., et al. (2019). Reduction in gray matter of cerebellum in schizophrenia and its influence on static and dynamic connectivity. *Human Brain Mapping, 40*(2), 517–528.
Ji, G. J., et al. (2019). Regional and network properties of white matter function in Parkinson's disease. *Human Brain Mapping, 40*(4), 1253–1263.
Jia, X., et al. (2019). Reconfiguration of dynamic large-scale brain network functional connectivity in generalized tonic-clonic seizures. *Human Brain Mapping, 41*(1), 67–79.
Jiang, Y., et al. (2019a). Aberrant prefrontal-thalamic-cerebellar circuit in schizophrenia and depression: Evidence from a possible causal connectivity. *International Journal of Neural Systems, 29*(5), 1850032.
Jiang, S., et al. (2018). Aberrant thalamocortical connectivity in juvenile myoclonic epilepsy. *International Journal of Neural Systems, 28*(1), 1750034.
Jiang, Y. C., et al. (2019b). White-matter functional networks changes in patients with schizophrenia. *NeuroImage, 190*, 172–181.
Jiang, Y. C., et al. (2019c). Dysfunctional white-matter networks in medicated and unmedicated benign epilepsy with centrotemporal spikes. *Human Brain Mapping, 40*(10), 3113–3124.
Kelly, C., et al. (2012). A convergent functional architecture of the insula emerges across imaging modalities. *NeuroImage, 61*(4), 1129–1142.
Klugah-Brown, B., et al. (2019a). Altered dynamic functional network connectivity in frontal lobe epilepsy. *Brain Topography, 32*(3), 394–404.
Klugah-Brown, B., et al. (2019b). Altered structural and causal connectivity in frontal lobe epilepsy. *Bmc Neurology*. https://doi.org/10.1186/s12883-019-1300-z
Kobayashi, E., et al. (2006). Temporal and extratemporal BOLD responses to temporal lobe interictal spikes. *Epilepsia, 47*(2), 343–354.
Kros, L., et al. (2015a). Controlling cerebellar output to treat refractory epilepsy. *Trends in Neurosciences, 38*(12), 787–799.
Kros, L., et al. (2015b). Cerebellar output controls generalized spike-and-wave discharge occurrence. *Annals of Neurology, 77*(6), 1027–1049.
Lange, T., et al. (2004). Stability-based validation of clustering solutions. *Neural Computation, 16*(6), 1299–1323.
Li, W., et al. (2019a). Different patterns of white matter changes after successful surgery of mesial temporal lobe epilepsy. *Neuroimage: Clinical, 21*, 101631.
Li, J., et al. (2019b). Exploring the functional connectome in white matter. *Human Brain Mapping, 40*(15), 4331–4344.
Li, H., et al. (2017). Reorganization of anterior and posterior hippocampal networks associated with memory performance in mesial temporal lobe epilepsy. *Clinical Neurophysiology, 128*(5), 830–838.
Lorio, S., et al. (2016). New tissue priors for improved automated classification of subcortical brain structures on MRI. *NeuroImage, 130*, 157–166.
Luo, C., et al. (2012). Disrupted functional brain connectivity in partial epilepsy: A resting-state fMRI study. *PLoS ONE, 7*(1), e28196.
Marussich, L., et al. (2017). Mapping white-matter functional organization at rest and during naturalistic visual perception. *NeuroImage, 146*, 1128–1141.
McDonald, C. R., et al. (2008). Subcortical and cerebellar atrophy in mesial temporal lobe epilepsy revealed by automatic segmentation. *Epilepsy Research, 79*(2–3), 130–138.
McIntyre, D. C., & Gilby, K. L. (2008). Mapping seizure pathways in the temporal lobe. *Epilepsia, 49*(Suppl 3), 23–30.
Morgan, V. L., Abou-Khalil, B., & Rogers, B. P. (2015). Evolution of functional connectivity of brain networks and their dynamic interaction in temporal lobe epilepsy. *Brain Connect, 5*(1), 35–44.
Morgan, V. L., et al. (2019). Divergent network properties that predict early surgical failure versus late recurrence in temporal lobe epilepsy. *Journal of Neurosurgery, 132*(5), 1324–1333.
Peer, M., et al. (2017). Evidence for functional networks within the human brain's white matter. *Journal of Neuroscience, 37*(27), 6394–6407.
Qin, Y., et al. (2019). BOLD-fMRI activity informed by network variation of scalp EEG in juvenile myoclonic epilepsy. *NeuroImage: Clinical, 22*, 101759.
Rodrigo, S., et al. (2007). Uncinate fasciculus fiber tracking in mesial temporal lobe epilepsy. Initial findings. *European Radiology, 17*(7), 1663–1668.
Schuck, N. W., et al. (2016). Human orbitofrontal cortex represents a cognitive map of state space. *Neuron, 91*(6), 1402–1412.
Tellez-Zenteno, J. F., & Hernandez-Ronquillo, L. (2012). A review of the epidemiology of temporal lobe epilepsy. *Epilepsy Research and Treatment, 2012*, 630853.
Tzourio-Mazoyer, N., et al. (2002). Automated anatomical labeling of activations in SPM using a macroscopic anatomical parcellation of the MNI MRI single-subject brain. *NeuroImage, 15*(1), 273–289.
Umeoka, S. C., et al. (2012). Requirement of longitudinal synchrony of epileptiform discharges in the hippocampus for seizure generation: A pilot study. *Journal of Neurosurgery, 116*(3), 513–524.
Voets, N. L., et al. (2012). Structural substrates for resting network disruption in temporal lobe epilepsy. *Brain, 135*, 2350–2357.
Wei, W., et al. (2016). more severe extratemporal damages in mesial temporal lobe epilepsy with hippocampal sclerosis than that with other lesions: A multimodality MRI study. *Medicine, 95*(10), e3020.
Wu, X., et al. (2017). Functional connectivity and activity of white matter in somatosensory pathways under tactile stimulations. *NeuroImage, 152*, 371–380.
Xu, S. W., et al. (2018). Cognitive decline and white matter changes in mesial temporal lobe epilepsy. *Medicine (Baltimore), 97*(33), e11803.
Yeo, B. T., et al. (2011). The organization of the human cerebral cortex estimated by intrinsic functional connectivity. *Journal of Neurophysiology, 106*(3), 1125–1165.
Zhou, X., et al. (2019). Disruption and lateralization of cerebellar-cerebral functional networks in right temporal lobe epilepsy: A resting-state fMRI study. *Epilepsy & Behavior, 96*, 80–86.
Zhu, X., et al. (2018). Altered spontaneous brain activity in MRI-negative refractory temporal lobe epilepsy patients with major depressive disorder: A resting-state fMRI study. *Journal of the Neurological Sciences, 386*, 29–35.